

Supersolids in the Bose-Hubbard Hamiltonian

G. G. Batrouni,¹ R. T. Scalettar,² G. T. Zimanyi,² and A. P. Kampf³

¹*Groupe Matière Condensée et Matériaux (URA 804), Université de Rennes I, 35042 Rennes CEDEX, France*

²*Physics Department, University of California, Davis, California 95616*

³*Institut für Theoretische Physik, Universität zu Köln, 50937 Köln, Germany*

(Received 18 April 1994; revised manuscript received 19 September 1994)

We use quantum Monte Carlo simulations to determine the ground state phase diagram of the Bose-Hubbard Hamiltonian with long-range repulsive interactions. At half filling one finds superfluidity and insulating solid phases. Depending on the relative sizes of near-neighbor and next-near-neighbor interactions, this solid follows either a checkerboard or a striped pattern. In neither case is there a coexistence with superfluidity. However, at incommensurate densities “supersolid” phases appear with simultaneous diagonal and off-diagonal long-range order.

PACS numbers: 67.40.Db, 05.30.Jp, 67.90.+z

Supersolids are defined by the simultaneous presence of *two types of long-range order*: superfluidity coexisting with a periodic modulation of the density. The concept of supersolids has been studied intensely for the past three decades. Yet even their very existence remains completely unresolved. Anderson argues against their existence [1], while previous papers of Andreev, Fisher, Leggett, and Nelson affirm it [2–6]. To date there is one promising experimental result indicating supersolidity in ⁴He [7], but the situation is controversial [8]. It is quite remarkable that in spite of these essential disagreements until recently there were no numerical studies aimed at settling the controversy. Our work provides exactly such a numerical analysis.

The issue at hand is very broad. Besides bosonic systems, there is a large class of electronic materials, such as NbSe₂ and A15 compounds, which form a charge density wave at higher temperatures, and which upon cooling exhibit a second, superconducting phase transition, thus defining the class of “fermionic supersolids.” Extensive Raman data are available on these materials [9], and the corresponding theories are well developed [10].

The possibility of supersolids naturally occurs in magnetic materials as well. Recalling that hard-core Bose systems map to spin-1/2 models, simultaneous ferromagnetic ordering in the *x-y* plane and antiferromagnetic ordering in the *z* direction is equivalent to a supersolid phase. The ordered phase of the Heisenberg model is a very clear example of this. A central theoretical issue is whether this coexistence at the special point of spin-rotational symmetry can be expanded to a finite region of the parameters by introducing additional couplings. These couplings may frustrate the Heisenberg system, giving rise to exotic phases besides the well-known Néel phase: a collinear phase with alternating lines of up and down spins [11], and disordered spin-liquid and dimer crystal phases [12]. The equivalent of the supersolid phase would further enrich this complex phase diagram.

Finally, studies of exotic phases in interacting boson models are closely related to other systems as well, for

example, to the Abrikosov phase in type-II superconductors [13]. Here the world lines of the bosons propagating in 2 + 1 dimensions map onto the flux lines of the three-dimensional bulk material. A recent paper explicitly identifies a supersolid phase in high *T_c* superconductors [14].

In the present work we report numerical investigations concerning supersolids. Our central result is that strong evidence favors the existence of supersolids in a broad range of parameters for incommensurate boson densities. In fact, we identify two types of supersolid phases, in analogy to the magnetic Néel and collinear phases.

We will explore the question of supersolid order within the context of the two-dimensional (2D) Bose-Hubbard Hamiltonian [15]

$$H = -t \sum_{\langle ij \rangle} (a_i^\dagger a_j + a_j^\dagger a_i) - \mu \sum_i n_i + V_0 \sum_i n_i^2 + V_1 \sum_{\langle ij \rangle} n_i n_j + V_2 \sum_{\langle\langle ik \rangle\rangle} n_i n_k. \quad (1)$$

Here a_i is a boson destruction operator at site i , and $n_i = a_i^\dagger a_i$. The transfer integral $t = 1$ sets the scale of the energy, and μ is the chemical potential. V_0, V_1 , and V_2 are on-site, near-neighbor, and next-near-neighbor boson-boson repulsions.

In the hard-core limit, the Bose-Hubbard Hamiltonian maps onto the quantum spin-1/2 Hamiltonian,

$$H = -t \sum_{\langle ij \rangle} (S_i^+ S_j^- + S_j^+ S_i^-) + V_1 \sum_{\langle ij \rangle} S_i^z S_j^z + V_2 \sum_{\langle\langle ik \rangle\rangle} S_i^z S_k^z - H_z \sum_i S_i^z. \quad (2)$$

The field $H_z = \mu - 2V_1 - 2V_2$. Ordering of the density corresponds to finite wave vector Ising-type order, whereas superfluidity is described by ferromagnetic ordering in the *X-Y* plane. The Heisenberg point is given by $V_1 = 2t, V_2 = H_z = 0$.

We begin with a brief review of the mean field phase diagram of Eq. (2) [16]. Increasing the density from

half filling the following phases can be expected: a Néel state, corresponding to a checkerboard Bose *solid* with an ordering vector $\mathbf{k}_* = (\pi, \pi)$; a ferromagnetic phase, with the net moment $M_{xy} \neq 0$ and $M_z \neq 0$, corresponding to a *superfluid*; and a fully polarized magnetic phase, where only $M_z \neq 0$, corresponding to a *Mott insulator*. As the solid and superfluid phases possess different broken symmetries, it is expected that the transition between them is first order. In an alternative scenario it was proposed that instead there could be two distinct second order transitions, where the two order parameters vanish at separate points [2,5,17]. In the regime between the two transitions *both* order parameters are nonzero; hence it has been termed a *supersolid* [4,16,17]. The mean field analysis revealed that long-range forces ($V_2 \neq 0$) are needed to stabilize the supersolid. Recently it was claimed that this conclusion changes in the soft-core case, and a supersolid phase exists with V_1 alone [18]. To gain an independent test of these results, we conducted numerical simulations of the problem.

Quantum simulations.—We have used the world line quantum Monte Carlo method. For details of the technique, see [20,21]. We work in the canonical ensemble, mostly near the special “half-filled” point $\rho = N_b/N = 1/2$. Solid ordering is demonstrated by measuring the equal time density-density correlations, and their Fourier transform, the structure factor, $S(\mathbf{k}) = \frac{1}{N} \sum_{\mathbf{j}, \mathbf{l}} e^{i\mathbf{k} \cdot (\mathbf{j} - \mathbf{l})} \langle n(\mathbf{j}, \tau) n(\mathbf{l}, \tau) \rangle$. Long-range solid order in the thermodynamic limit is signaled by a linear growth of $S(\mathbf{k}_*)$ with the number of lattice sites, N , at some ordering vector \mathbf{k}_* . In Eq. (1), V_1 drives the formation of a checkerboard phase with $\mathbf{k}_* = (\pi, \pi)$, where sites are alternately empty and occupied, an Ising-type Néel antiferromagnet in the spin language. V_2 favors a striped phase where *lines* of occupied sites in either the x or y direction alternate with *lines* of empty sites. In this case the structure factor peaks at either $\mathbf{k}_* = (0, \pi)$ or $(\pi, 0)$. We will measure the superfluid density by looking at a topological property of the boson world lines, the winding number [20,21].

One can determine the ground state phase diagram either by simulating lattices with large β or else by appropriately scaling $\beta \propto L^z$ with linear spatial lattice size L . Here z is the dynamic critical exponent. The latter technique assumes foreknowledge of z which is later justified by appropriate scaling behavior, but has advantages in the precise determination of phase boundaries. We shall use it for that purpose when required. However, as has been done extensively in simulations of both fermion [22] and boson [20] systems, we will primarily choose β large enough so that $\xi > L$ and so observables no longer change and we are assured of measuring ground state properties.

Results at half filling.—Our first question is whether the supersolid phase can exist without a finite V_2 [18,23]. Figure 1 shows the staggered structure factor $S(\pi, \pi)$

and superfluid density ρ_s as a function of near-neighbor interaction strength V_1 at $V_0 = 7$ and $V_2 = 0$. We see a sharp transition in both quantities at $V_1 \approx 2.5$. The raw data already strongly suggest that there is no supersolid phase intervening between the superfluid and solid. We performed the appropriate finite size scaling analysis and found that the transition points differ by at most 0.5%, which we regard as statistically insignificant. We also tried to drive the supersolid by turning on V_2 near the transition found in Fig. 1. Therefore we studied $S(\pi, \pi)$, $S(\pi, 0)$, $S(0, \pi)$, and ρ_s at $V_0 = 7$, $V_1 = 2.75$ (i.e., just inside the solid phase), sweeping V_2 . We found that V_2 induces a nonzero value of ρ_s while simultaneously destroying the checkerboard order. For $V_2 > V_1/2$ we enter the striped solid phase [$S(\pi, 0) \neq 0$], and again ρ_s vanishes. Supersolids were not found anywhere in the phase diagram.

We have also explored a case of very soft-core bosons where $V_0 = 3$. At $V_2 = 0$ a transition from a superfluid (SF) to checkerboard solid occurs at $V_1 = 3.35$, with no supersolid in between. Nor does turning on V_2 help create one. Our conclusion is that, in agreement with mean field theory, and contrary to what has recently been found [23], no supersolid phase exists at $\rho = 1/2$ in the Bose-Hubbard model.

Supersolids in the defect phase.—We turn next to the doped phase where $\delta = \rho - 1/2 \neq 0$. In Fig. 2 we show a plot of ρ_s and $S(\pi, \pi)$ vs V_1 at $V_2 = 0$ and $\delta = 0.03$. We see that a tail of nonzero ρ_s persists beyond the point where the solid has formed. Figure 3 contains data for two lattice sizes, 8×8 and 10×10 , at the same doping, demonstrating that the tail is not a finite size effect. We have also studied 12×12 lattices, establishing this point conclusively. ρ_s drops considerably, but remains nonzero, as the supersolid is entered. Our picture is that $N_b = N/2$ bosons freeze into a solid, leaving only the remaining bosons mobile. These then condense into a superfluid proportional to δ , indicating that indeed only defect bosons make up the superfluid condensate within

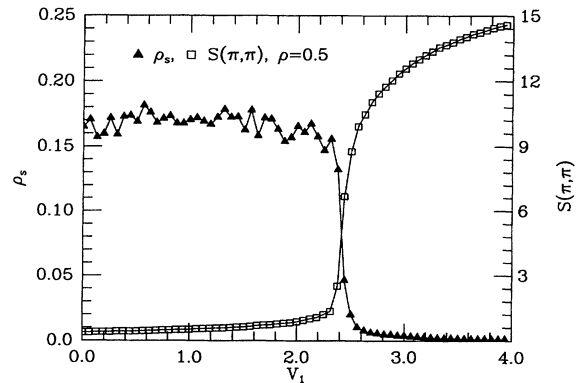


FIG. 1. ρ_s and $S(\pi, \pi)$ are shown for $V_0 = 7$, $V_2 = 0$.

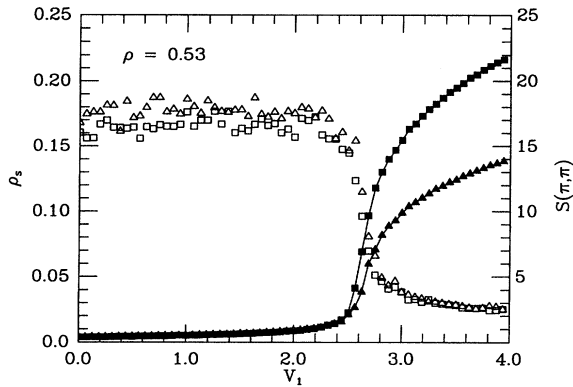


FIG. 2. ρ_s and $S(\pi, \pi)$ are shown at $V_0 = 7.0, V_2 = 0.0$.

the solid. Systems with densities up to $\rho \approx 0.675$ exhibit a supersolid phase, further doping destroys the diagonal long-range order and drives a transition into a pure superfluid phase. $S(\pi, \pi)$ scales linearly with lattice size, thus long-range crystalline order is indeed present in the checkerboard supersolid.

Figure 2 exhibits the superfluid in coexistence with the checkerboard solid. One can also get superfluidity in a striped solid phase. This is illustrated in Fig. 3 where we show $S(\pi, 0)$, $S(0, \pi)$, and ρ_s at $V_0 = 7, V_1 = 2.75$, and $\delta = 0.06$ as a function of V_2 . At small V_2 we are in the superfluid phase, where all the bosons participate in the condensate. At larger V_2 the striped supersolid emerges. Note that in Fig. 3 we separately plot the superfluid fraction in the x and y directions. In the checkerboard supersolid and in the pure superfluid we find $\rho_{sx} = \rho_{sy}$. However, in the striped supersolid this rotational symmetry is broken and $\rho_{sx} \neq \rho_{sy}$. The symmetry is broken randomly in the different runs, and there is the expected correlation between ρ_{sx} [ρ_{sy}], and which of $S(\pi, 0)$ [$S(0, \pi)$] is large. *The one-dimensional superfluid flows down only the appropriate channels left open by the striped solid phase.* The boson wave function is localized in the orthogonal direction. However, there is

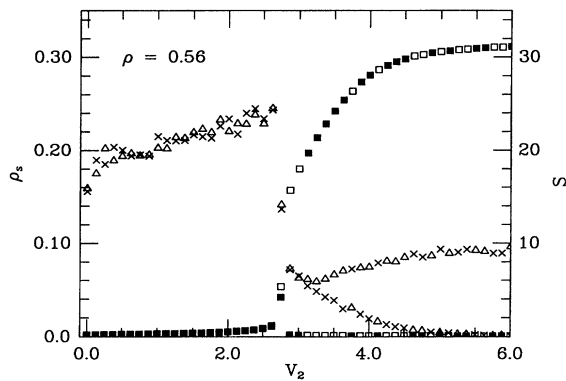


FIG. 3. ρ_s , $S(\pi, 0)$, and $S(0, \pi)$ are shown at $V_0 = 7.0, V_1 = 2.75$.

an exponentially small overlap between the wave functions of different rows, giving rise to a small but nonzero stiffness also in the perpendicular direction. This effect is so small that the Monte Carlo results cannot resolve it.

Sweeps of V_1 and V_2 in the hard-core case give the phase diagram in Fig. 4 for $\rho = 0.56$. At weak couplings we have a superfluid phase, while at strong couplings two types of supersolids emerge, following the checkerboard and striped patterns. The superfluid phase extends out along the strong coupling line $V_2 = V_1/2$ in a very robust manner, as opposed to the situation in 1D, where the superfluid window was rather narrow [24]. This is a consequence of the highly degenerate nature of the strong coupling ($t = 0$) ground state. As can easily be seen, not only do the Néel and checkerboard solids have the same energy, but an infinite number of defect states are degenerate as well. For example, in a horizontally aligned collinear solid a whole column can be shifted up and down without energy cost [25]. This large degeneracy stabilizes superfluidity, even at large coupling. At $\rho = 0.5$, we find that along the strong coupling line the superfluid phase vanishes around $V_1 = 6$.

The phase diagram shown in Fig. 4 has important connections to the behavior of the J_1 - J_2 Heisenberg Hamiltonian [11,12]. In this model, the addition of a frustrating next-near-neighbor J_2 interaction drives a transition from an ordered Néel state to a quantum disordered phase. Further increase of J_2 promotes collinear order, and it is believed that there is no intervening superfluid phase between the two solids. We find instead a superfluid existing along the strong coupling line. This arises because our J_2 couples only the z components of spin. Order in the x - y plane, and hence superfluidity is not frustrated.

For our zero temperature *quantum* phase transition, the static periodic potential of solid bosons does *not* confine defects in the Néel supersolid. The wave functions of the defect or doped bosons are extended Bloch states, thus they can condense into a superfluid phase. A doped boson can move either through an intermediate state of double

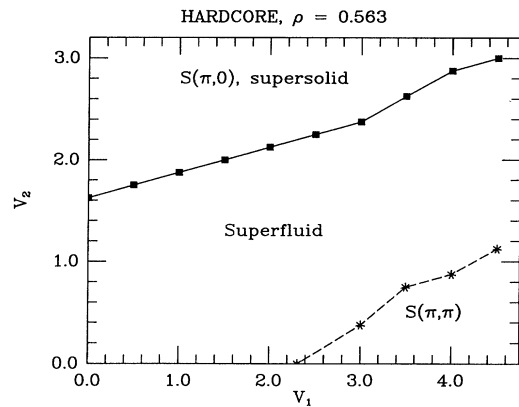


FIG. 4. The ground state phase diagram of the BH model at half filling.

occupation of energy cost $\Delta = V_0$ or through a move of two neighboring bosons of energy cost $\Delta = 2V_1$. The excess bosons have extended superfluid wave functions with a mass renormalized to $m_* = \sqrt{1 + (\Delta/16t)^2}/2t$ from the bare $m = 1/2t$. This value for m_* comes from considering a single noninteracting boson moving over the rigid "solid" of background bosons, with alternating 0 and Δ site energies. That bosons can move in the solid without double occupancy explains that the supersolid is present in the hard-core limit as well. Meanwhile, in the striped supersolid, the doped bosons move entirely freely along the lines of unoccupied sites. We find ρ_s is larger by about a factor of 2 in the striped supersolid than in the Néel supersolid at the same doping.

We note that we have studied a lattice model, whereas in the bulk helium problem there is no such underlying periodic potential. Thus the relevance of our results for the continuum case is limited and a direct continuum formalism is needed to study supersolids in bulk helium. However, our results *do apply* naturally for helium on substrates, and predict the existence of supersolid phases. It is as yet unclear whether this scenario for supersolids is realized experimentally. There is one positive [7] and numerous negative experiments in bulk ^4He [8]. Some thin film studies indicate the existence of superfluidity in incomplete layers on top of close-packed solid ones [2]. In this situation one might imagine though that *different* layers are giving rise to the two types of order, rather than a single layer being both solid and superfluid.

In conclusion, we studied the formation of supersolid phases in interacting boson systems. Strong correlations lead to the formation of Néel and collinear solid phases. Defects introduced into these solid do not destroy the diagonal long-range order, but rather Bose condense into a superfluid. These supersolid phases, instead of existing in some narrow range of the parameter space, are a rather generic feature of the Bose-Hubbard model.

We acknowledge useful discussions with D. Arovas. This work was supported by National Science Foundation Grant DMR 92-06023 and by Thinking Machines Corporation. A. P. K. gratefully acknowledges support through a habilitation scholarship of the Deutsche Forschungsgemeinschaft.

[1] P. W. Anderson, *Basic Notions in Condensed Matter Physics* (Benjamin, New York, 1984), p. 152.

[2] A. F. Andreev, in *Progress in Low Temperature Physics*,

edited by D. G. Brewer (North-Holland, Amsterdam, 1982), Vol. VIII.

- [3] A. F. Andreev and I. M. Lifshitz, *Sov. Phys. JETP* **29**, 1107 (1969).
- [4] K. S. Liu and M. E. Fisher, *J. Low Temp. Phys.* **10**, 655 (1973).
- [5] A. J. Leggett, *Phys. Rev. Lett.* **25**, 1543 (1970).
- [6] D. Nelson and M. E. Fisher, *Phys. Rev. Lett.* **32**, 1350 (1974).
- [7] G. A. Lengua and J. M. Goodkind, *J. Low Temp. Phys.* **79**, 251 (1990).
- [8] M. W. Meisel, *Physica (Utrecht)* **178**, 121 (1992), and references therein.
- [9] R. Sooryakumar and M. Klein, *Phys. Rev. Lett.* **45**, 660 (1980).
- [10] G. Bilbro and W. L. Mcmillan, *Phys. Rev. B* **14**, 1887 (1976); P. B. Littlewood and C. M. Varma, *Phys. Rev. Lett.* **47**, 81 (1981); I. Tutto and A. Zawadowski, *Phys. Rev. B* **45**, 4842 (1992).
- [11] P. Chandra, P. Coleman, and A. Larkin, *J. Phys. Condens. Matter* **2**, 7933 (1990).
- [12] N. Read and S. Sachdev, *Phys. Rev. Lett.* **66**, 1773 (1991); F. Figuerido *et al.*, *Phys. Rev. B* **41**, 4619 (1990); R. R. P. Singh and R. Narayanan, *Phys. Rev. Lett.* **65**, 1072 (1990); E. Dagotto and A. Moreo, *Phys. Rev. Lett.* **63**, 2148 (1989).
- [13] M. P. A. Fisher and D. H. Lee, *Phys. Rev. B* **39**, 2756 (1989).
- [14] E. Frey, D. Nelson, and D. S. Fisher, *Phys. Rev. B* **49**, 9723 (1994).
- [15] M. P. A. Fisher, P. B. Weichman, G. Grinstein, and D. S. Fisher, *Phys. Rev. B* **40**, 546 (1989).
- [16] H. Matsuda and T. Tsuneto, *Suppl. Prog. Theor. Phys.* **46**, 411 (1970).
- [17] G. Chester, *Phys. Rev. A* **2**, 256 (1970).
- [18] E. Roddick and D. H. Stroud, *Phys. Rev. B* **40**, 16600 (1993).
- [19] J. E. Hirsch, R. L. Sugar, D. J. Scalapino, and R. Blankenbecler, *Phys. Rev. B* **26**, 5033 (1982).
- [20] G. G. Batrouni, R. T. Scalettar, and G. T. Zimanyi, *Phys. Rev. Lett.* **65**, 1765 (1990).
- [21] E. L. Pollock and D. M. Ceperley, *Phys. Rev. B* **36**, 8343 (1987).
- [22] J. E. Hirsch and S. Tang, *Phys. Rev. Lett.* **62**, 591 (1989); S. R. White, D. J. Scalapino, R. L. Sugar, E. Y. Loh, J. E. Gubernatis, and R. T. Scalettar, *Phys. Rev. B* **40**, 506 (1989).
- [23] A. van Otterlo and K.-H. Wagenblast, *Phys. Rev. Lett.* **72**, 3598 (1994).
- [24] P. Niyaz, R. T. Scalettar, C. Y. Fong, and G. G. Batrouni, *Phys. Rev. B* **44**, 7143 (1991).
- [25] U. Brandt, *Z. Phys. B* **53**, 283 (1983).